Search for $K^+ \to \pi^+ \nu\bar{\nu}$ at NA62

M Perrin-Terrin on behalf of the NA62 Collaboration[1] CERN, Switzerland

E-mail: mathieu.perrin-terrin@cern.ch

Abstract. The $K^+ \to \pi^+ \nu\bar{\nu}$ branching ratio is one of the key observables to test the Standard Model. The NA62 experiment has been designed to measure this branching ratio with a 10% precision. Most of the experiment systems have been commissioned during 2014 and 2015 runs and physics data have been recorded. The analysis of this data shows performances close to the nominal ones.

[1] for the NA62 Collaboration:
G. Aglieri Rinella, R. Aliberti, F. Ambrosino, R. Ammendola, B. Angelucci, A. Antonelli, G. Anzivino, R. Arcidiacono, I. Azhinenko, S. Balev, M. Barbanera, J. Bendotti, A. Biagioni, L. Bician, C. Biino, A. Bizzeti, T. Blazek, A. Blik, B. Bloch-Devaux, V. Bolotov, V. Bonaiuto, M. Boretto, M. Bragadireanu, D. Britton, G. Britvich, M.B. Brunetti, D. Bryman, F. Bucci, F. Butin, E. Capitolo, C. Capoccia, T. Capussela, A. Cassese, A. Catinaccio, A. Cecchetti, A. Ceccucci, P. Cenci, V. Cerny, C. Cerri, B. Checcucci, O. Chikilev, S. Chiozzi, R. Ciaranfi, G. Collazuol, A. Conovaloff, P. Cooke, P. Cooper, G. Corradi, E. Cortina Gil, F. Costantini, F. Cotorobai, A. Cotta Ramusino, D. Coward, G. D'Agostini, J. Dainton, P. Dalpiaz, H. Danielsson, J. Degrange, N. De Simone, D. Di Filippo, L. Di Lella, S. Di Lorenzo, N. Dixon, N. Doble, B. Dobrich, V. Duk, V. Elsha, J. Engelfried, T. Enik, N. Estrada, V. Falaleev, R. Fantechi, V. Fascianelli, L. Federici, S. Fedotov, M. Fiorini, J. Fry, J. Fu, A. Fucci, L. Fulton, S. Gallorini, S. Galeotti, E. Gamberini, L. Gatignon, G. Georgiev, A. Gianoli, M. Giorgi, S. Giudici, L. Glonti, A. Goncalves Martins, F. Gonnella, E. Goudzovski, R. Guida, E. Gushchin, F. Hahn, B. Hallgren, H. Heath, F. Herman, T. Husek, O. Hutanu, D. Hutchcroft, L. Iacobuzio, E. Iacopini, E. Imbergamo, O. Jamet, P. Jarron, E. Jones, T. Jones K. Kampf, J. Kaplon, V. Kekelidze, S. Kholodenko, G. Khoriauli, A. Khotyantsev, A. Khudyakov, Yu. Kiryushin, A. Kleimenova, K. Kleinknecht, A. Kluge, M. Koval, V. Kozhuharov, M. Krivda, Z. Kucerova, Yu. Kudenko, J. Kunze, G. Lamanna, G. Latino, C. Lazzeroni, G. Lehmann-Miotto, R. Lenci, M. Lenti, E. Leonardi, P. Lichard, R. Lietava, L. Litov, R. Lollini, D. Lomidze, A. Lonardo, M. Lupi, N. Lurkin, K. McCormick, D. Madigozhin, G. Maire, C. Mandeiro, I. Mannelli, G. Mannocchi, A. Mapelli, F. Marchetto, R. Marchevski, S. Martellotti, P. Massarotti, K. Massri, P. Matak, E. Maurice, A. Mefodev, E. Menichetti, E. Minucci, M. Mirra, M. Misheva, N. Molokanova, J. Morant, M. Morel, M. Moulson, S. Movchan, D. Munday, M. Napolitano, I. Neri, F. Newson, A. Norton, M. Noy, G. Nuessle, T. Numao, V. Obraztsov, A. Ostankov, S. Padolski, R. Page, V. Palladino, G. Paoluzzi, C. Parkinson, E. Pedreschi, M. Pepe, F. Perez Gomez, M. Perrin-Terrin, L. Peruzzo, P. Petrov, F. Petrucci, R. Piandani, M. Piccini, D. Pietreanu, J. Pinzino, I. Polenkevich, L. Pontisso, Yu. Potrebenikov, D. Protopopescu, F. Raffaelli, M. Raggi, P. Riedler, A. Romano, P. Rubin, G. Ruggiero, V. Russo, V. Ryjov, A. Salamon, G. Salina, V. Samsonov, C. Santoni, G. Saracino, F. Sargeni, V. Semenov, A. Sergi, M. Serra, A. Shaikhiev, S. Shkarovskiy, I. Skillicorn, D. Soldi, A. Sotnikov, V. Sugonyaev, M. Sozzi, T. Spadaro, F. Spinella, R. Staley, A. Sturgess, P. Sutcliffe, N. Szilasi, D. Tagnani, S. Trilov, M. Valdata-Nappi, P. Valente, M. Vasile, T. Vassilieva, B. Velghe, M. Veltri, S. Venditti, P. Vicini, R. Volpe, M. Vormstein, H. Wahl, R. Wanke, P. Wertelaers, A. Winhart, R. Winston, B. Wrona, O. Yushchenko, M. Zamkovsky, A. Zinchenko.

1. Introduction

The $K^+ \to \pi^+ \nu\bar{\nu}$ decay occurs in the Standard Model mainly through the electroweak penguin and box diagrams such as the ones represented in Figure 1.

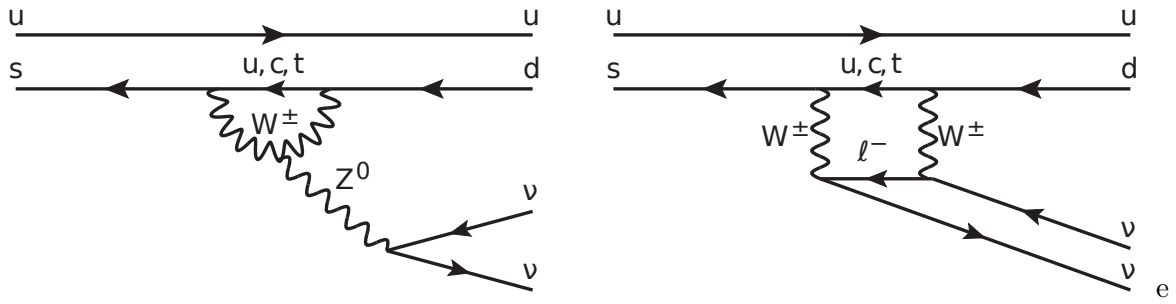

Figure 1. Examples of electroweak penguin and box Feynman diagrams contributing to $K^+ \to \pi^+ \nu\bar{\nu}$ in the SM.

These diagrams are suppressed by the Glashow-Iliopoulos-Maiani mechanism and by the Cabibbo-Kobayashi-Maskawa (CKM) off-diagonal matrix elements $V_{is}^{\star} V_{id}$. Hence the decay is very rare in the SM, its branching ratio is [1]

$$\begin{aligned} \mathcal{B}(K^+ \to \pi^+ \nu\bar{\nu}) &= (8.4 \pm 0.3) \times 10^{-11} \left(\frac{|V_{cb}|}{0.0407}\right)^{2.8} \left(\frac{\gamma}{73.2}\right)^{0.74} \\ &= (8.4 \pm 1.0) \times 10^{-11}. \end{aligned}$$

The precision of this prediction is remarkably good and dominated by the uncertainties on the external CKM parameters $|V_{cb}|$ and γ, one of the angle of the CKM triangle. The pure theoretical uncertainties is below 4%. Such a precision is achievable as the transition is dominated by perturbatively computable short-range processes, the Feynman diagrams with the top quark loop, for which the hadronic matrix elements can be derived from the well measured $K^+ \to \pi^0 e^+ \nu$ branching ratio.

The $K^+ \to \pi^+ \nu\bar{\nu}$ decay branching ratio allows to probe physics beyond the SM. Several recent publications [1, 2] highlighted the sensitivity of the decay up to mass scales as high as 100 TeV as well as its interplay with other observables being currently measured. For example, the correlation between the branching ratios of $K^+ \to \pi^+ \nu\bar{\nu}$ and $K_L \to \pi^0 \nu\bar{\nu}$ is one of the theoretically cleanest bench mark to probe the SM, as most of the CKM parametric uncertainties affecting the two branching ratios cancels in their correlation. A similar cancellation happens in the correlation between the branching ratios of $K^+ \to \pi^+ \nu\bar{\nu}$ and $B_s^0 \to \mu^+ \mu^-$ [1].

Experimentally, measuring such a rare decay with only one charged track in the final state is a real challenge. Searches for $K^+ \to \pi^+ \nu\bar{\nu}$ have started decades ago and the most sensitive analysis, published by the E949 Collaboration [3], gives a value of

$$\mathcal{B}(K^+ \to \pi^+ \nu\bar{\nu}) = (17.3^{+11.5}_{-10.5}) \times 10^{-11}. \quad (1)$$

The NA62 Collaboration aims at measuring the decay branching ratio with a 10% precision with the data that will be collected by the end of 2018. After a pilot run in 2014, the experiment is taking physics data since 2015.

2. Experimental Strategy

2.1. The NA62 Apparatus

The NA62 experiment [4] is installed in the CERN North Area at the SPS and schematically represented in Figure 2.

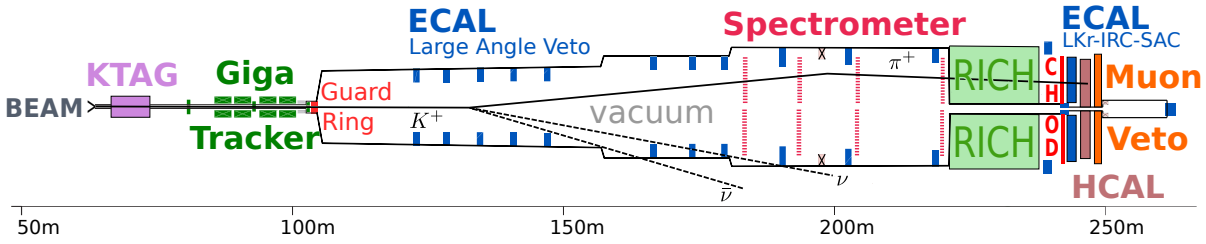

Figure 2. Schematic view of the NA62 experiment, excluding the beam line.

Assuming a 10% signal acceptance and a signal to background ratio of 10/1, the experiment needs to collect 10^{13} K^+ decay. The beam line was designed to meet this goal using the 400 GeV protons from a SPS beam line. The beam entering the experiment is un-separated and composed at 70% of protons, 24% of π^+'s and 6% of K^+'s with a total instantaneous nominal particle rate of 750 MHz. The beam particle momentum distribution peaks at 75 GeV and its standard deviation is 1%. The SPS extraction line delivers continuous spills during few seconds and operates in cycles with duty factors of around 20%. The experiment and the beam line compose a 300 m long evacuated tank with a pressure of 10^{-6} mbar reaching diameters up to almost 4 meters. In the downstream region the tank is instrumented with two sets of detectors measuring either the beam particles or the decay products properties. The beam being continuous, all detectors must also provide sub nanosecond timing information. In order to achieve the 12 orders of magnitude of background suppression needed for the measurement, the experiment employs many independent experimental techniques.

The K^+ in the beam are identified by the KTAG, a nitrogen differential Cherenkov detector. The momentum and directions of all beam particles are measured with the GigaTracker (GTK) made of three 3×6 cm^2 thin planes of time-resolved silicon hybrid pixels. The beam then enters the 100 m long decay region. In order to reduce the background induced by inelastic collisions in the last GTK plane, a guard ring of scintillators is installed downstream of the GTK to collect hits from the collisions fragments.

The most abundant background source is the $K^+ \to \pi^+\pi^0$ decay where the γ from the π^0 are missed. The experimental challenge is to reduce the inefficiency on γ from by 8 orders of magnitude. To reach this goal an electromagnetic calorimeter (ECAL) has been designed to to detect at least one of these two γ up to 50 mrad. The ECAL is made of four subsystems. Photons with polar angles between 8.5 and 50 mrad are detected with the 12 ring lead-glass Large Angle Vetoes (LAV). The Liquid Krypton Calorimeter (LKr) covers the region between 8.5 mrad and 1 mrad. The inner edges of the LKr hole along the beam line are covered by a shashlik calorimeter called Inner Radius Calorimeter (IRC). Finally another shashlik calorimeter called Small Angle Calorimeter is installed at the end of the beam line, downstream of a bending magnet sweeping away the un-decayed beam particles and covers the angular region down to 0 mrad. The direction and momentum of the charged decay products are measured by a magnetic straw tube spectrometer operating inside the vacuum tank. The charged decay products are timed with 200 ps resolution by a fast array of scintillators called Charged Hodoscope (CHOD). The identification of the decay products are obtained by three systems: a ring imaging Cherenkov detector filled with neon at atmospheric pressure; a hadronic calorimeter (HCAL) made of two layers of iron-scintillator sandwiches, and finally a muon veto installed behind a iron wall and made of fast scintillators.

The experiment data acquisition system employs a multi-layer trigger system. At the lowest level, hits time in the CHOD, RICH and MUV and, calorimetric variables in the LKr and HCAL are computed using FPGA's.These data are sent to a central processor, operating also

on FPGA, that builds and issues trigger requests upon which the state of all detectors, but LKr and GTK, in the time window corresponding to the trigger are readout. Based on the detectors states, algorithms running on a PC farm issue refined trigger requests upon which the remaining detectors are readout and the event assembled and stored.

In 2015 the hardware and readout of the detectors have been commissioned with a beam intensity of 10% of the nominal one. The beam line has however been commissioned up to nominal intensity. The GigaTracker was running with a partial hardware configuration. Data have been collected with a $K^+ \to \pi^+\nu\bar{\nu}$ trigger using the calorimetric variables at L0 and with a minimum bias trigger based on the CHOD timing. Section 3, describes the analysis of the minimum bias sample in view of the $K^+ \to \pi^+\nu\bar{\nu}$ branching ratio measurement.

2.2. Analysis Strategy

The signal signature consists of an isolated π^+ track making a good vertex with a K^+ track. Two main sources of events can mimic this signal: the incorrectly reconstructed K^+ decays and the beam activity. The analysis is performed using the candidate square missing mass, define as:

$$m_m \quad = \quad |p_{K^+} - p_{\pi^+}|^2, \tag{2}$$

where p_{K^+} and p_{π^+} are the 4-momenta of the mother and daughter particles under the K^+ and π^+ mass hypothesis. The distribution of this variable for the main K^+ decay modes and for the signal is shown in Figure 3. The signal candidates are sought in the two regions around the $K^+ \to \pi^+\pi^0$ missing mass peak and among the candidates with a downstream track momentum between 15 and 35 GeV. To suppress further the remaining backgrounds, kinematics, timing, photon rejection and particle identification are needed.

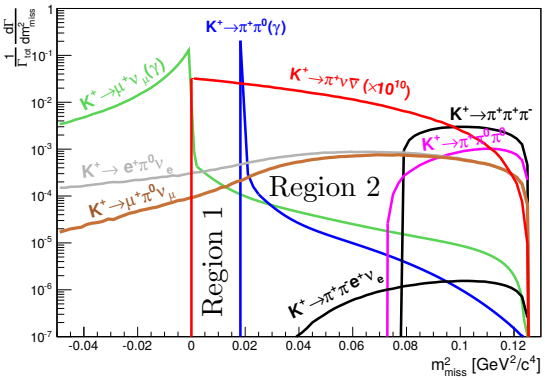

Figure 3. Squared missing mass theoretical distribution of the main K^+ decays and the $K^+ \to \pi^+\nu\bar{\nu}$ decay normalised by their branching ratios. The $K^+ \to \pi^+\nu\bar{\nu}$ distribution is scaled by 10 orders of magnitude.

3. Performance in view of the 2015 minimum bias data

This section presents an analysis of data collected in 2015 with the minimum bias trigger in view of assessing the detector performance for the $K^+ \to \pi^+\nu\bar{\nu}$ analysis. The kinematics, particle identification and photon rejection are assessed using a sample of single track events.

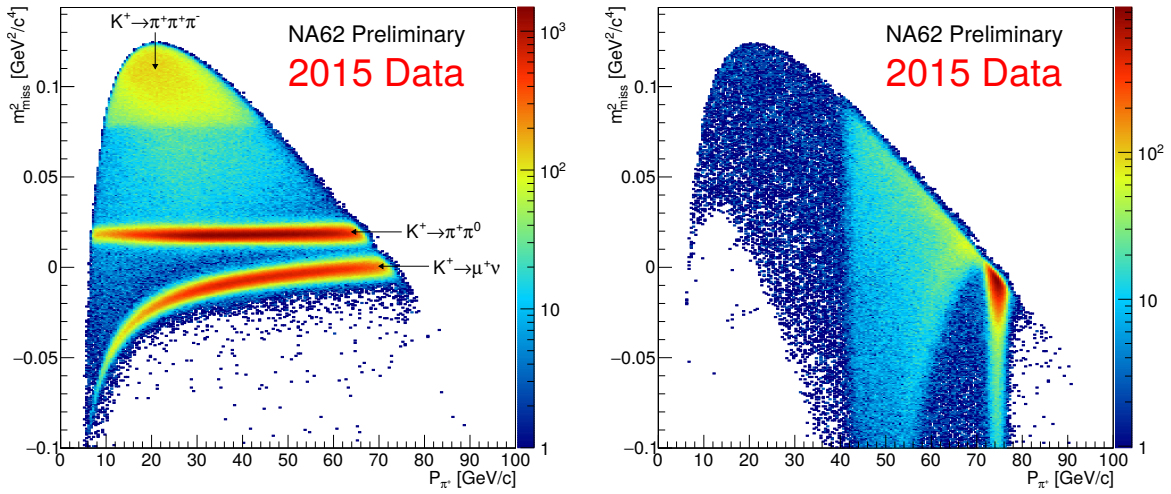

Figure 4. Squared missing mass distribution as a function of the straw tack momentum for the single track events with the GTK track identified (left) or not identified (right) as a K^+ by the KTAG.

3.1. Single Track Events

The signal signature consists of a isolated π^+ track making a good vertex with a K^+ track. Hence signal candidates are selected asking for a good isolated spectrometer track, matched in space with energy depositions in the calorimeters and with a hit in the CHOD. The track is isolated if no other spectrometer tracks form a good vertex with it inside the fiducial decay region defined as the 65m long region between the last GTK station the the first spectrometer plane. In addition this track is requested to make a good vertex with a GTK track and its associated CHOD hit to be in time with a KTAG candidate. The squared missing mass of the selected candidates as a function of the spectrometer track momentum is shown in Figure 4 left.

Reverting the positive KTAG identification allows to study the beam activity. The distribution in Figure 4 right shows that the beam activity consists mainly of beam π^+ decay, beam particle elastic scattering and inelastic scattering in the last GTK plane. This beam activity is suppressed thanks to the good time resolution of the CHOD, KTAG and GTK measured to 200, 100 and 200 ps respectively, in agreement with the nominal design.

3.2. Kinematics Performance

The control of the resolution of the $K^+ \to \pi^+\pi^0$ squared missing mass peak is essential to reduce the tails entering in the two signal regions. This resolution is measured to be around 1.2×10^{-3} GeV^2/c^4, close to the design value (1.0×10^{-3} GeV^2/c^4). Note that without the GTK momentum measurement, i.e. assuming the nominal beam parameters, this resolution is three times larger.

The kinematics $K^+ \to \pi^+\pi^0$ background suppression in the signal region can be evaluated with a pure sample of $K^+ \to \pi^+\pi^0$ selected from the previous single track events with the additional requirement of having two π^0 γ's in the LKr. A background suppression of 10^{-3} is found while the nominal one is 10^{-4}. The discrepancy is understood to be caused by the partial GTK hardware setup leading to mis-reconstructed tracks.

3.3. Particle Identification Performance
The particle identification system has to provide a rejection factor of 10^{-7} for $\mathsf{K}^+ \to \mu^+\nu$ on top of the kinematic rejection. The π^+/μ^+ separation is evaluated using the previous $\mathsf{K}^+ \to \pi^+\pi^0$ sample and a $\mathsf{K}^+ \to \mu^+\nu$ sample selected from the single track event asking a hit in the MUV. With the 2015 mirrors alignment, the RICH allows to get a 10^{-2} μ^+ rejection for a 80% π^+ efficiency for track momenta between 15 and 35 GeV/c. Efficiencies closer to 90% are expected to be reached once the mirrors will be realigned. The background suppression from the calorimeter is under investigation. Simple cut based technique allows to reach a 10^{-4} to 10^{-6} μ^+ rejection for a 90% to 50% π^+ efficiency.

3.4. Photon Vetoes Performance
The photon veto system has to provide a rejection factor of 10^{-8} on π^0 from for $\mathsf{K}^+ \to \pi^+\pi^0$. The momentum cut on the π^+ below 35 GeV/c insures that the π^0 has at least a momentum of 40 GeV/c and is emitted forward. Hence the single γ rejection in the angular region below 50 mrad has only to be 10^{-5} for γ's with energies above 10 GeV. The rejection factor is measured using the $\mathsf{K}^+ \to \pi^+\pi^0$ selected within the single track event. The measurement of the $\mathsf{K}^+ \to \pi^+\pi^0$ rejection is statistically limited and the rejection is found to be at least 10^{-6} at 90% CL. The effect of random veto on the signal is measured using $\mathsf{K}^+ \to \mu^+\nu$ and scattered beam π^+'s and leads to a signal efficiency of 90%.

4. Conclusions and Prospects
The $\mathsf{K}^+ \to \pi^+\nu\bar{\nu}$ branching ratio is one of the key observables to test the SM. The NA62 experiment is designed to measured its branching ratio with a 10% precision. The experiment is built and most of the systems have been commissioned. The data taken in 2015 shows performances close to the design sensitivity to measure $\mathsf{K}^+ \to \pi^+\nu\bar{\nu}$. Refined analyses are on going and data taking has restarted in April 2016.

5. References
[1] A. J. Buras, D. Buttazzo, J. Girrbach-Noe, R. Knegjens, $K^+ \to \pi^+\nu\overline{\nu}$ and $K_L \to \pi^0\nu\overline{\nu}$ in the Standard Model: status and perspectives, Journal of High Energy Physics 11 (2015) 033. arXiv:1503.02693.
[2] A. J. Buras, D. Buttazzo, J. Girrbach-Noe, R. Knegjens, Can we reach the Zeptouniverse with rare K and $B_{s,d}$ decays?, Journal of High Energy Physics 11 (2014) 121. arXiv:1408.0728.
[3] The E949 Collaboration, Study of the decay $K^+ \to \pi^+\nu\bar{\nu}$ in the momentum region $140 < P_\pi < 199$ MeV/c, Physical Review D79 (2009) 092004. arXiv:0903.0030.
[4] The NA62 Collaboration, NA62: Technical Design Document, NA62-10-07.